

DECAY ANGULAR DISTRIBUTIONS OF $p\pi^-$ STATES FORMED IN DIFFRACTION DISSOCIATION OF NEUTRONS ON CARBON*

J.C. VANDER VELDE, L.W. JONES, M.J. LONGO and D.D. O'BRIEN
University of Michigan, Ann Arbor, Michigan 48104

M.B. DAVIS**, B.G. GIBBARD*** and M.N. KREISLER
Princeton University, Princeton, New Jersey 08540

Received 13 December 1971
(Revised 26 May 1972)

Abstract: We present decay angular distributions of the $p\pi^-$ system formed from the interactions of 25–30 GeV/c neutrons on a carbon target. The data are studied as a function of t' , which allows a partial separation of coherent and incoherent events. It is found that the coherent production goes substantially into $p\pi^-$ states with $J \geq \frac{3}{2}$ and is consistent with pure $J = \frac{3}{2}$. We are not able to draw any firm conclusions about the question of helicity conservation from the data. There is no evidence for coherent production of the known $I = \frac{1}{2}$ resonances. Comparison is made of the data with predictions of the Drell-Hiida-Deck and double Regge models. In their present form these models do not appear to give satisfactory descriptions of the data.

1. INTRODUCTION

In a spark chamber experiment at the Brookhaven AGS we have studied the process

$$n + A \rightarrow p + \pi^- + A', \quad (1)$$

where A and A' represent a target and recoiling nucleus respectively. A description of the beam, the apparatus, and results for the mass and t' distributions for various nuclei have been given previously [1]. The salient features of the results were a broad low-mass peak in the $p\pi^-$ system with essentially no evidence for resonances and a sharp forward peak in the $t(n \rightarrow p\pi^-)$ distribution characteristic of coherent diffractive production.

* Work supported in part by the US National Science Foundation and the US Atomic Energy Commission.

** N.D.E.A. Predoctoral Fellow.

*** Now at CERN, Geneva 23, Switzerland.

In the present paper we discuss the decay angular distributions of the $p\pi^-$ system produced off a carbon target. We restrict the data to neutron momenta in the range 25–30 GeV/c. The data for lower momenta and other targets are not significantly different from those presented.

2. DECAY ANGULAR DISTRIBUTIONS

We have analyzed the decay angular distributions in two coordinate frames defined in the $p\pi^-$ c.m.s.. In the Jackson frame the \hat{z} axis is taken along the incident neutron direction, or the direction of a virtual particle exchanged in the t -channel. In the helicity frame the \hat{z} axis is opposite to that of the recoiling nucleus, or the direction of a virtual particle exchanged in the s -channel. The two frames coincide at $t' \equiv t - t_{\min} = 0$. In both frames the \hat{y} axis is perpendicular to the production plane ($\hat{y} \equiv \vec{A} \times \vec{A}'$).

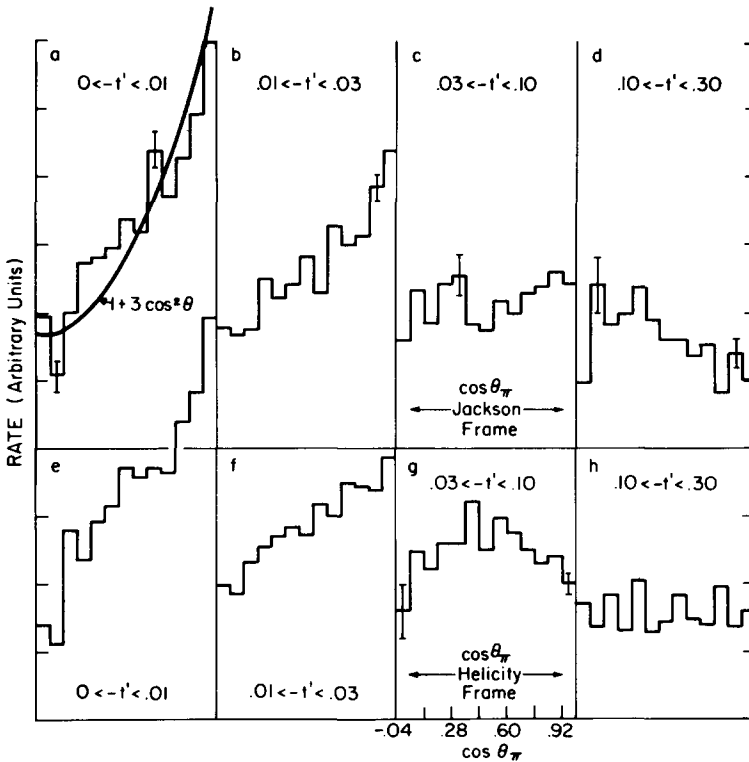


Fig. 1. Distributions in the cosine of the polar angle of the π^- in the $p\pi^-$ rest frame. a–d are for various t' bins as indicated and θ is measured in the Jackson frame. e–h are for the same t' bins with θ measured in the helicity frame. Note that all distributions only cover the angular range $-0.04 < \cos \theta < 1.0$. The $p\pi^-$ invariant mass is restricted to the interval 1.10–1.32 GeV. The higher mass region gives similar results.

The distributions of the cosine of the polar angle of the π^- in these systems are shown in fig. 1. The data are divided into four t' intervals, where t' is the four-momentum transfer squared minus its minimum value. We believe that the lowest t' interval contains primarily coherent events, the second interval about half coherent events, and the highest two intervals primarily incoherent events. The precise coherent/incoherent ratio for each interval is unknown since we do not observe the state of the recoiling nucleus and therefore must rely on the shape of the t' distribution to indicate the fraction of coherent events [1]. The distributions, which have been corrected for detection efficiency, have been cut off at $\cos \theta = -0.04$ in each case because our efficiency becomes small beyond that point. Thus we only present that half of the angular range in which the π^- goes forward in the $p\pi^-$ rest frame.

3. DISCUSSION OF SPIN STATES

Referring to fig. 1 (a or e) there is a definite peaking toward $\cos \theta = +1$. This is characteristic of a $p\pi^-$ system with spin $J \geq \frac{3}{2}$ which is restricted by kinematics to have helicity values of $\pm \frac{1}{2}$ at $t' = 0$. In fact, at $t' = 0$ we expect a flat distribution for pure $J = \frac{1}{2}$, and $(1 + 3 \cos^2 \theta)$ for pure $J = \frac{3}{2}$ [2]. As J increases one gets a steeper and steeper peak and a broader and flatter minimum [3]. As can be seen from the curve on fig. 1a the data are fairly well represented by a pure $J = \frac{3}{2}$ state, although a mixture of several spins cannot be ruled out. If we assume, for the moment, that an arbitrary mixture of $J = \frac{1}{2}$ and $J = \frac{3}{2}$ is all that is present for $-t' < 0.01$, then $\geq 70\%$ of the cross section is due to $J = \frac{3}{2}$, if we allow no interference.

If we assume that only $J = \frac{1}{2}$ states are present then the $\frac{1}{2}^+$ P wave and $\frac{1}{2}^-$ S wave amplitudes can interfere to give an angular distribution of the form $1 + B \cos \theta$ where B has a maximum value of 1. Such a distribution fits the data rather poorly so that at least some $J \geq \frac{3}{2}$ amplitude must be present. If we allow only S and P waves so that the three amplitudes $\frac{1}{2}^+$, $\frac{1}{2}^-$, and $\frac{3}{2}^+$ are possible, then the data require a minimum of about 15% $\frac{3}{2}^+$ amplitude with maximum constructive interference. In fact, 20% $\frac{3}{2}^+$ amplitude can interfere with 80% $\frac{1}{2}^+$ to give the same $1 + 3 \cos^2 \theta$ shape as pure $J = \frac{3}{2}$. Thus we cannot rule out a mixed state which is predominantly $J = \frac{1}{2}$. However, the constancy of the angular distribution as a function of mass, shown in fig. 3, would seem to make this explanation unlikely since rather small changes in the relative amplitudes and phases of interfering states can cause rapid fluctuations in the angular distributions. In any case the calculations of Rushbrooke and of Resnick [4] which predict overwhelming dominance of $J = \frac{1}{2}$ seem not to be borne out.

The simplest interpretation of the data would be a cross section in the low t' region which was dominated by $\Delta J \geq 1$ or possibly pure $\Delta J = 1$. We note that the dissociation on heavy targets of π into A_1 and K into Q mesons seem to show a similar $\Delta J = 1$ behavior [5], so that one is tempted to speculate that this is a general property of diffraction dissociation. We emphasize, however, that our data are

consistent with a mixture of several different J^P states, including $J = \frac{1}{2}$. We have no information about the parity of the $p\pi^-$ system.

4. DISCUSSION OF HELICITY CONSERVATION

We turn now to the question of helicity conservation [6]. Recent data on rho photoproduction and π -N elastic scattering [7] have indicated s -channel helicity is conserved for these processes, whereas t -channel helicity appears to be conserved in the reaction $\pi p \rightarrow A_1 p$ [8].

For the reaction we are studying, helicity conservation in the t -channel (s -channel) over a given t' interval, would imply that the $\cos \theta$ distributions were independent of t' in the Jackson (helicity) coordinate frame, *provided* a pure J^P state was being produced or the various amplitudes in a mixed state had the same t' dependence. Since we have no reason to make such assumptions, the rapid t' dependence of the shapes of the $\cos \theta$ distributions shown in fig. 1 do not rule out helicity conservation in either channel.

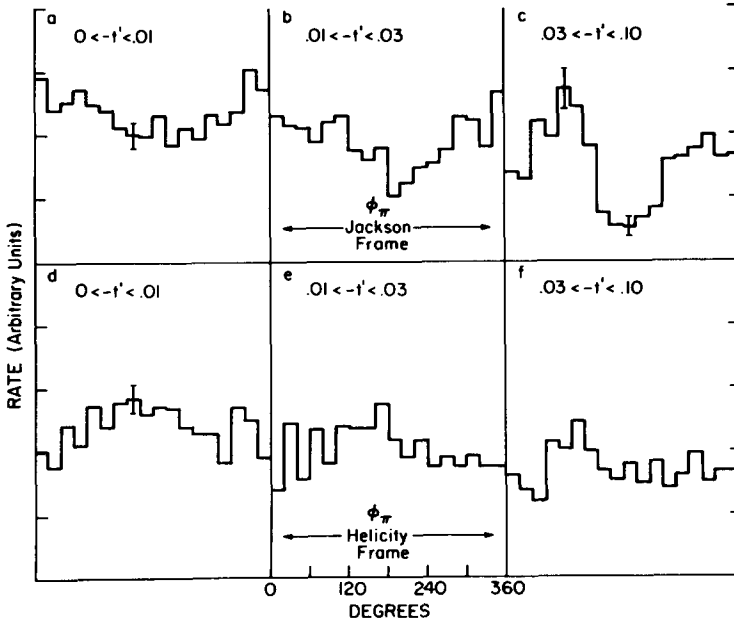


Fig. 2. Distributions in the azimuthal angle of the π^- in the $p\pi^-$ rest frame. a-c are for the Jackson frame and d-f for the helicity frame in various t' bins as noted. In a-c only those events with $\cos \theta$ (Jackson) ≥ 0 are plotted and in d-f only those events with $\cos \theta$ (helicity) ≥ 0 are plotted. The $p\pi^-$ mass is in the interval 1.10–1.32 GeV. The higher mass region gives similar results.

It is possible that the $\cos \theta$ distributions are separately independent of t' for coherent and incoherent events, i.e. a peaked $\cos \theta$ distribution (fig. 1a) for coherent production could be superimposed on a relatively flat distribution (fig. 1d) for incoherent production, with both processes being t' -independent and adding to give the intermediate distributions of figs. 1b and 1c.

For the azimuthal angle distributions, t -channel (s -channel) helicity conservation implies a flat distribution in the Jackson (helicity) frame. Since we have an unpolarized beam and target, the distributions *must* be flat at $t' = 0$. The helicity frame distributions (figs. 2d–f) are consistent with being flat for all t' and therefore allow (but do not require) helicity conservation in the s -channel for both the incoherent and coherent events. The anisotropy in fig. 2c appears to rule out t -channel helicity conservation for incoherent events but we hesitate to conclude that this implies the same would be true for a free nucleon target. The incoherent background could be responsible for the slight anisotropy in figs. 2a and 2b so that t -channel helicity conservation cannot be ruled out for the coherent production. Thus we cannot draw any firm conclusions about helicity conservation from our data. The question could perhaps be settled if it were possible to obtain a much cleaner sample of coherent events than ours. It would also be instructive to know the production and decay characteristics on hydrogen.

5. COMPARISON WITH MODELS

Based on the structureless mass distribution, it was noted in ref. [1] that there is very little, if any, evidence for production of resonances in the low t' region. The angular distributions in fig. 3 seem to confirm this. They show no change as one moves through the entire mass region, including that of the known $I = \frac{1}{2} \pi^- p$ resonances in the interval 1400–1700 MeV. The entire coherent cross section appears to arise from a single mechanism which is mass-independent except for rate.

We have attempted to describe the data with various models based on the diagram shown in fig. 4a. In the Drell-Hiida-Deck (D-H-D) model [9] the shaded blob is represented by a phenomenological π^- -C elastic diffraction scattering. The cross section is given by [9]

$$\frac{d^4\sigma}{dt dM^2 d(\cos \theta) d\varphi} \propto \left(\frac{P^*}{M}\right) e^{\lambda t} (S_1^2) \frac{(-\Delta^2)}{(\Delta^2 - \mu^2)^2} F(\Delta^2), \quad (2)$$

where θ , φ , and P^* are measured in the $\pi^- p$ rest frame and M is the $\pi^- p$ invariant mass. The slope $\lambda \approx 50 \text{ GeV}^{-2}$ for carbon, and the variable $S_1^2 = 0.25 \times (S_{\pi C} - (M_C + \mu)^2)(S_{\pi C} - (M_C - \mu)^2)$ with $S_{\pi C}$ being the π^- -C' invariant mass, and M_C and μ the carbon and pion masses. The form factor $F(\Delta^2)$ can be an arbitrary (presumably decreasing) function of the n to p four-momentum transfer Δ .

This D-H-D form for the cross section does not give a good fit to the data, for any

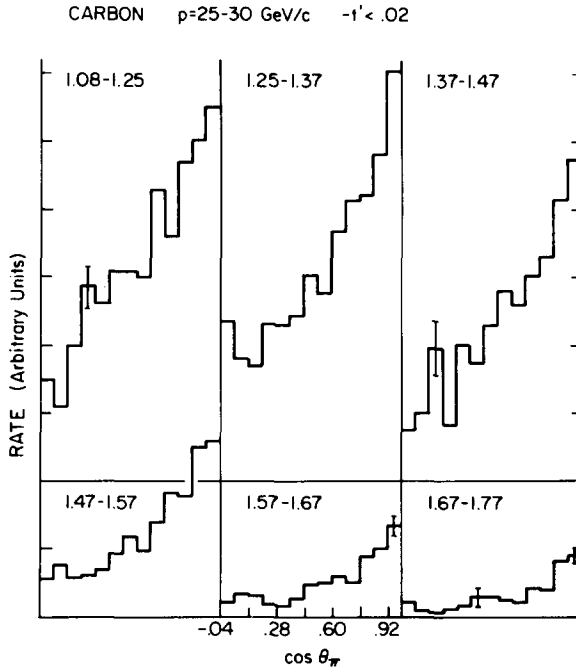


Fig. 3. $\cos \theta$ distributions (Jackson frame) for $-t' < 0.02$ as a function of $p\pi^-$ mass, as labeled. Note that all distributions only cover the angular range $-0.04 < \cos \theta < 1.0$.

$F(\Delta^2)$, for the following reason. If we put $F = 1$ then the predicted mass spectrum peaks at too high a mass and is too broad, as can be seen in fig. 4b. Moreover the prediction for the $\cos \theta_\pi$ (Jackson) distribution is approximately proportional to $(1 + \cos \theta_\pi)$ for small t' . This is a poor fit to the data which, as has been shown, is closer to $1 + 3 \cos^2 \theta_\pi$. If we now change $F(\Delta^2)$ to be a decreasing function in order to fit the mass spectrum, then the $\cos \theta_\pi$ predictions is even *less* peaked toward $\cos \theta_\pi = +1$ and the $\cos \theta_\pi$ fit becomes worse. *Thus the D-H-D model cannot be made to fit the mass spectrum and the $\cos \theta$ spectrum simultaneously, even for an arbitrary $F(\Delta^2)$.* Incidentally, putting $F = -1/\Delta^2$ gives a mass peak much too low and sharp, as can be seen in fig. 4b. This F also predicts an approximately flat $\cos \theta$ distribution.

The other model we have tried is the Reggeized version of the D-H-D model as suggested by Berger [10]. In this model the exchanged particles of fig. 4a are to be represented by the pion and the Pomernanchukon Regge trajectories. The essential difference between the formula we use for this double Regge Model (DRM) and the D-H-D model is the replacement in (2) of $F(\Delta^2)$ by

$$F_2(\Delta^2, M) = \left[\frac{M^2 - m^2 + \frac{1}{2}\Delta^2}{S_{20}} \right]^{2\alpha_\pi},$$

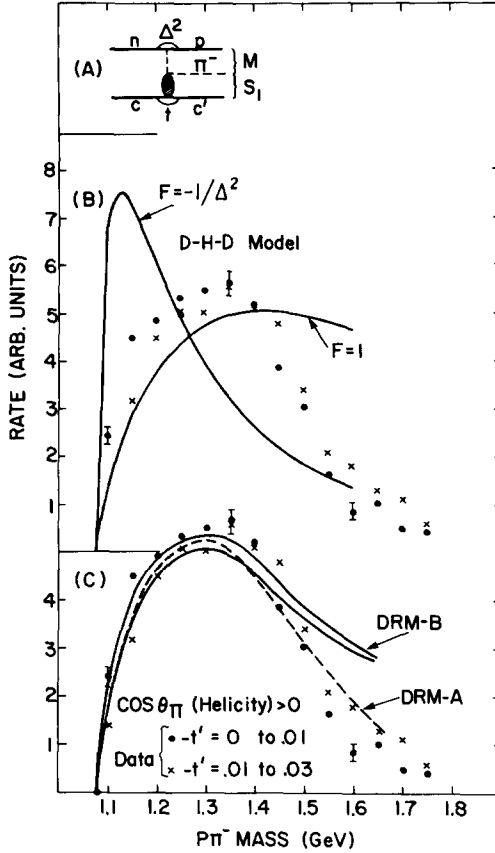


Fig. 4. (a) Exchange diagram for Drell-Hiida-Deck or double Regge models. (b) $p\pi^-$ mass spectrum. Solid curves are predictions of D-H-D model, for two different form factors, in the $-t'$ interval 0.0 to 0.01 GeV^2 . (c) $p\pi^-$ mass spectrum predictions for DRM-A and DRM-B (see text). Both the data and the theoretical curves in (b) and (c) are restricted to $\cos \theta_\pi$ (helicity) > 0. Data have been corrected for detection efficiency.

where m is the neutron mass, S_{20} is an unknown scale constant, and $\alpha_\pi(\Delta^2)$ is the pion Regge trajectory. We will discuss two different choices of α_π and S_{20} which give approximate agreement with the data. Both choices have a linear pion trajectory, $\alpha_\pi = \alpha_0 + \alpha' \Delta^2$ with $\alpha' = 1.0 \text{ GeV}^{-2}$. In the first choice (DRM-A) we put $\alpha_0 = -0.02$ and $S_{20} = 0.7 \text{ GeV}^2$. The second choice (DRM-B) has $\alpha_0 = -0.5$ and $S_{20} = 1.8 \text{ GeV}^2$. This second choice for α_π does not seem consistent with what is known about the pion trajectory but, as we will show, it gives a significantly better fit to the data than choice A does. Thus DRM-A should be viewed as the simplest version of the model, whereas DRM-B at this point represents just a change in the parameters in such a way as to give better agreement with the data, but does not

necessarily make any good physical sense in the context of the DRM. These two choices by no means exhaust all the possible parameter sets or modifications of the DRM, but they represent about the best one can do in fitting our data using eqs. (2) and (3), and perhaps this is instructive.

If we look first at the mass spectrum (fig.4c) we see that the factor F_2 brings the theory into reasonable agreement with the data for both DRM-A and DRM-B. Note that both data and theory include only the region $\cos \theta_\pi$ (helicity) > 0 . The t' dependence of DRM-B is indicated by the upper and lower curves for the $-t'$ intervals of (0 to 0.01) and (0.01 to 0.03) respectively. DRM-A shows a similar behavior but the $-t' = (0.01 \text{ to } 0.03)$ prediction is omitted for clarity.

The *relative normalization* of the predictions for the two t' intervals is only approximately meaningful in the sense that we have multiplied the prediction for the higher $-t'$ interval by a factor of 2.0 to account for the data in this interval being approximately 50% background. We will consistently use this relative normalization when plotting predictions for angular distributions in the remainder of the paper.

In plotting angular distributions we now divide the data into four subsets defined by the two mass intervals $\Delta M_1 = 1.10 \text{ to } 1.32 \text{ GeV}$, $\Delta M_2 = 1.32 \text{ to } 1.56 \text{ GeV}$; and the two $-t'$ intervals $\Delta t'_1 = 0.0 \text{ to } 0.01 \text{ GeV}^2$, $\Delta t'_2 = 0.01 \text{ to } 0.03 \text{ GeV}^2$.

The distributions of $\cos \theta_\pi$ (Jackson) are shown in fig. 5. The normalizations are determined from the ΔM_1 , $\Delta t'_1$ interval in each case. The choice DRM-B gives a significantly better description than DRM-A, particularly in the ΔM_2 interval.

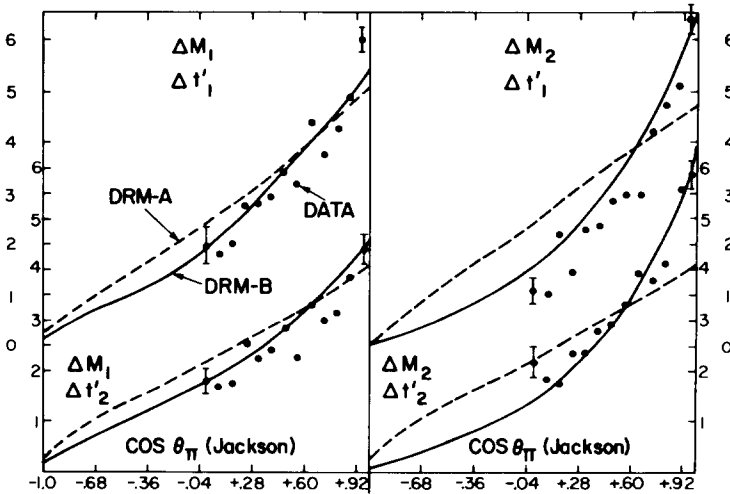


Fig. 5. Distributions of $\cos \theta_\pi$ (Jackson) for four different mass and t' intervals as described in text. The data are given by the solid dots and some typical error bars are shown. Predictions of DRM-A and DRM-B are given by dashed and solid curves respectively. The normalizations are described in the text. The ordinates are in arbitrary units.

We next look at the azimuthal distributions in the Jackson frame, shown in fig. 6. In this case both DRM-A and DRM-B give fairly acceptable fits. The drop-off of the theories toward $\varphi = 180^\circ$ is due to the S_1^2 factor in (2), which explicitly violates t -channel helicity conservation. Clearly the data taken as a whole also show such a violation. However, as mentioned earlier, we cannot be sure that the *coherent* events by themselves would show a violation.

The distributions in φ_π (helicity) are shown in fig. 7. The data here are almost flat, showing only a slight upward trend toward 180° . The DRM-B appears to give a better description of the data than does DRM-A, as was the case in fig. 5.

To summarize, the Drell-Hiida-Deck formula (2) does not give an adequate description of our data, even for an arbitrary choice of $F(\Delta^2)$. The factor $F_2(\Delta^2, M)$ of the double Regge Model allows a somewhat better description of the data, but with the following shortcomings. The DRM-A (normal pion trajectory) does *not* give a good description of the $\cos \theta$ and φ (helicity) distributions. We note that by arbitrarily changing the pion intercept to -0.5 one can improve the $\cos \theta$ and φ (helicity) fits but it is not clear that this makes any physical sense. Within the context of the DRM it might mean that a combination of the pion trajectory plus lower lying ones and possible Regge cuts is needed to describe diffraction dissociation. It would be of

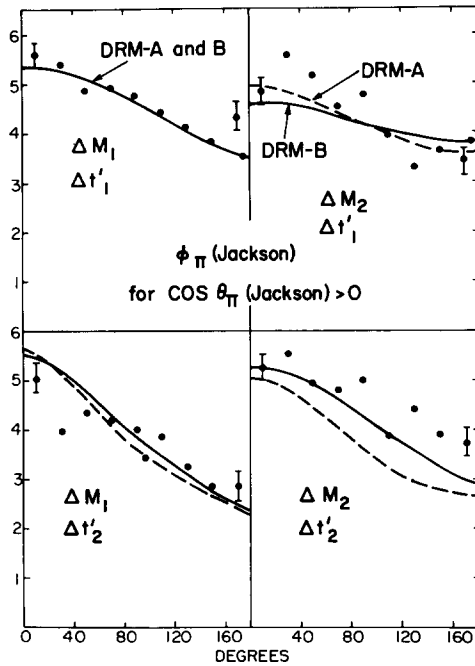


Fig. 6. Distributions of azimuthal angle in the Jackson frame for four different mass and t' intervals. Data are given by solid dots. Predictions of DRM-A and DRM-B are shown by dashed and solid curves respectively.

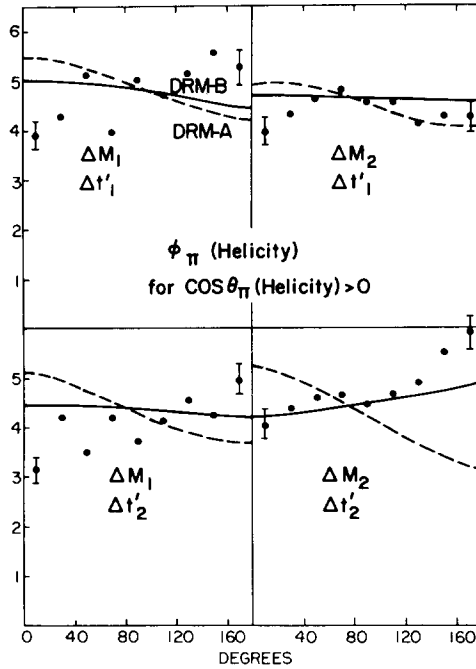


Fig. 7. Distributions of azimuthal angle in the helicity frame for four different mass and t' intervals. Data are given by solid dots. Predictions of DRM-A and DRM-B are shown by dashed and solid curves respectively.

interest to pursue these questions further with data which covers the whole $\cos \theta$ region and a wider t range than ours do. Applicability to a variety of reactions would also seem essential for any model to be believable.

We would like to thank G. Kane, M. Ross and J. Pumplin for helpful discussions.

REFERENCES

- [1] M.J. Longo et al., Phys. Letters 36B (1971) 560.
- [2] K. Gottfried and J.D. Jackson, Nuovo Cimento 33 (1964) 309.
- [3] The exact distributions were provided to us by G. Kane, private communication.
- [4] J.G. Rushbrooke, Phys. Rev. 177 (1969) 2357;
L. Resnick, Phys. Rev. 150 (1966) 1292.
- [5] H.H. Bingham, Review of coherent multiparticle production reactions from nuclei, CERN report D. Ph. II/PHYS/70-60;
D.R.O. Morrison, Diffraction dissociation and pomeron exchange, CERN report D. Ph. II/PHYS/70-64;
other references can be found in the above papers.

- [6] F.J. Gilman et al., *Phys. Letters* 31B (1970) 387;
G. Cohen-Tannoudji et al., *Phys. Letters* 33 B(1970) 183;
R. Silver, Tests for helicity conservation and spin parity selection rules in diffraction dissociation, Caltech preprint CALT-68-284 (1970).
- [7] J. Ballam et al., *Phys. Rev. Letters* 24 (1970) 960;
V. Barger and R.J.N. Phillips, *Phys. Letters* 26B (1968) 730.
- [8] J.V. Beaupre et al., *Phys. Letters* 34B (1971) 160;
G. Ascoli et al., *Phys. Rev. Letters* 26 (1971) 929.
- [9] S. Drell and K. Hiida, *Phys. Rev. Letters* 7 (1961) 199;
R.T. Deck, *Phys. Rev. Letters* 13 (1964) 169.
- [10] E.L. Berger, *Phys. Rev.* 179 (1969) 1567, and *Phys. Rev. Letters* 21 (1968) 701.